



ELSEVIER

Available online at [www.sciencedirect.com](http://www.sciencedirect.com)

International Communications in Heat and Mass Transfer xx (2008) xxx–xxx

**International Communications in  
HEAT and MASS  
TRANSFER**
[www.elsevier.com/locate/ichmt](http://www.elsevier.com/locate/ichmt)

# Shrinkage study of textile roller molded by conventional/microcellular injection-molding process <sup>☆</sup>

Shyh-shin Hwang <sup>a,\*</sup>, Peming P. Hsu <sup>b</sup>, Chi-wei Chiang <sup>a</sup>

<sup>a</sup> Department of Mechanical Engineering, Ching-Yun University, Chung-Li, 32023, Taiwan, ROC

<sup>b</sup> Department of Mechanical Engineering, Far-East University, Tainan, 74420, Taiwan, ROC

## Abstract

One of the advantages of microcellular conventional injection molding over conventional injection molding is that the shrinkage of the part can be reduced. This project investigated the effect of the process parameters on the shrinkage of the textile roller by conventional/microcellular injection-molding process. Polybutyleneterephthalate (PBT) materials with 30 wt.% glass and Wollastonite fiber were used. The results showed that the shrinkage by microcellular injection molding is less than that of conventional injection molding. Glass fiber filled PBT has more shrinkage than Wollastonite fiber filled PBT due to the non-uniform cell size of the glass fiber filled PBT.

© 2008 Published by Elsevier Ltd.

*Keywords:* Microcellular injection molding; Three-plate-mold; PBT; Glass fiber; Wollastonite; Shrinkage

## 1. Introduction

The microcellular process was first introduced by N. P. Suh [1,2] as a batch process in 1980. In this process, a polymer sample is housed in a high pressure chamber. An inert gas like CO<sub>2</sub> or N<sub>2</sub> is introduced into the chamber, diffusing into the polymer until saturation. Then, the pressure is rapidly reduced while the polymer temperature is simultaneously increased, producing a thermodynamic instability that lowers the gas solubility and creates cell growth. The disadvantage of the batch process is that a long period of time is required for the polymer to become saturated with the gas, due to low diffusion rates at room temperature. To avoid this problem, microcellular extrusion was developed. It reduces the time necessary for the gas to saturate the polymer by introducing the inert gas into the barrel while the polymer is still molten. The diffusion rate is high because the temperature in the barrel is high. Unfortunately, as parts become more complex, microcellular extrusion cannot be used to produce them.

In response, microcellular injection molding was developed [3] and commercialized by Trexel Co. Ltd. as the Mucell<sup>®</sup> process. The key insight of this process is the application of a

supercritical fluid. The supercritical fluid is injected during the injection stage cycle, creating millions of micron-sized voids in otherwise solid thermoplastic polymer parts.

Several studies have investigated the shrinkage and warpage of injection molded parts. Bushko et al. [4,5] studied the effect of processing conditions on shrinkage, warpage, and residual stresses of a thermal viscoelastic melt. Their results showed that a higher packing pressure resulted in less shrinkage. Liao et al. [6] investigated optimal process conditions for shrinkage and warpage in thin-wall parts. They showed that the optimal process conditions differ for shrinkage and warpage in injected thin-wall cellular-phone covers. Recently, Kramschuster et al. [7] studied the shrinkage and warpage behavior of a grocery box in microcellular and conventional injection molding. They showed that the SCF level and injection speed are the most important factors affecting the shrinkage and warpage of microcellular injection molded parts. In the author's last paper [8], we have showed that the shrinkage rate of microcellular injection molding is less than that of convention injection molding.

The textile roller (Fig. 1) in the textile machines is a worn part which should be replaced after a certain time. The material of the roller is PBT. PBT has good dimensional stability, mechanical strength, stiffness, and fire retardant characteristics. To improve the mechanical strength, most of the plastics are filled with glass fiber. In this study, both glass and Wollastonite fiber filled PBT

<sup>☆</sup> Communicated by W.J. Minkowycz.

\* Corresponding author.

E-mail address: [stanhwang@cyu.edu.tw](mailto:stanhwang@cyu.edu.tw) (S. Hwang).

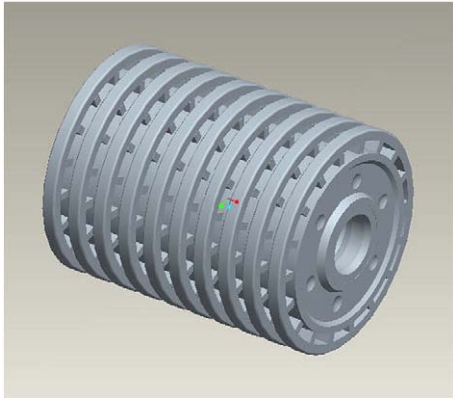


Fig. 1. Simplified diagram of textile roller.

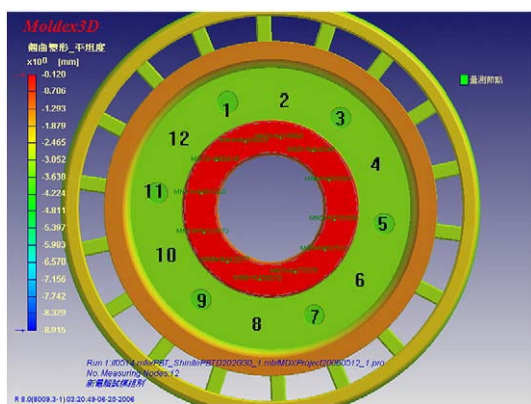


Fig. 2. Points 1, 3, 5, 7, 9 and 11 are the gate positions. The rim thickness is measured at red area according to the 12 points direction from center. (For interpretation of the references to colour in this figure legend, the reader is referred to the web version of this article.)

In this study, we have investigated the effects of process parameters on the variation of the rim thickness (Fig. 2) by conventional and microcellular injection molding. The specification of the rim thickness is  $\pm 0.02$  mm. If the rim thickness tolerance is out of specification, there is a running noise from the roller, and the textile roller should be replaced after a certain time.

## 2. Experimental work

### 2.1. Material

The materials used were 30 wt.% glass fiber filled PBT and 30 wt.% Wollastonite fiber filled PBT. The PBT material, Shinte D202G30, was supplied by Shinkong Synthetic Fibers Co. The material was dried at 120 °C for 3 h before injection molding. The PVT diagram [10] is shown in Fig. 3.

### 2.2. Part geometry and mold design

A three-plate-mold with 4 cavities of a textile roller was used in this study. Each cavity has six gates around the thin section of the roller (Fig. 4). Points 1, 3, 5, 7, 9 and 11 are the gate positions (Fig. 2). There is a weld-line in between 1 and 3 and so on. The rim thickness of the textile roller is 6.4 mm in the cavity.

### 2.3. Injection-molding machine

The injection-molding machine used was the Arburg 420C Allrounder 1000-350, equipped with Mucell capability. Nitrogen is used as the gas source. In this study, the process parameters; melt temperature, injection speed, shot size, melt plastification pressure (MPP), SCF level, and mold temperature; were varied to determine the effects on the rim thickness of the textile roller. The details of the process parameters are shown in Table 1.

Experiments were carried out by changing one factor at a time and keeping the others constant. The rim thickness was measured by micrometer, and the microstructure of the foamed part was examined by scanning electron microscope (SEM).

### 2.4. Microscopy

A SEM was used to observe the morphology of the cell structure in the textile roller. The cell structure in the SEM image was taken on a JEOL

are investigated. Wollastonite is a calcium metasilicate ( $\text{CaSiO}_3$ ) which can improve thermal and dimensional stability at elevated temperatures [9].

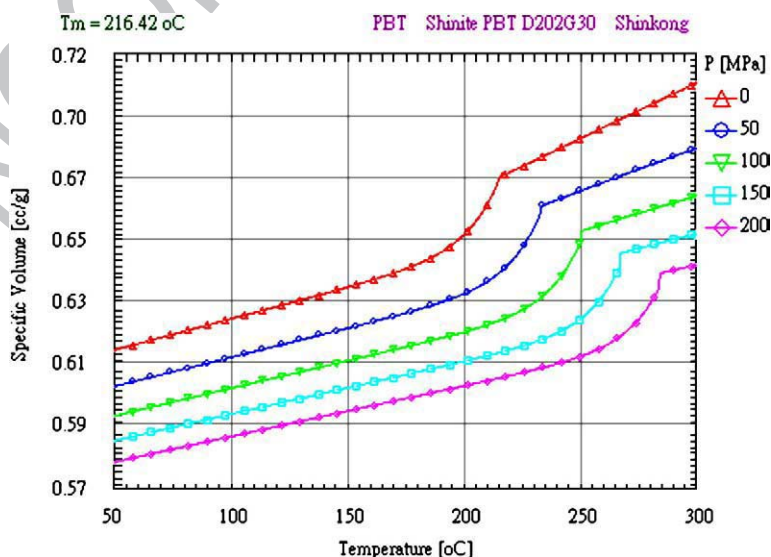


Fig. 3. PVT diagram of the glass fiber filled PBT material [10].



Fig. 4. The configuration of sprue, runner and gate.



Fig. 5. Short shot of the four cavities.

JSM6360. Specimens were cut into smaller pieces and gold was sputtered onto the surface. They were then inspected using the SEM.

### 3. Results and discussions

Although there are 4 cavities in one mold, only one cavity (#1 in Fig. 5) was taken for the measurement in order to get consistent data. The rim thickness was the average of the five samples. The experiment was carried out by short shot first and showed that the runner system has unbalanced melt flow problem (Fig. 5) [11]. Some portions are filled whereas some are only partially filled. To improve this problem, a modified mold design is needed which will be mentioned later. The injection-molding process was done by the conventional method first, and then the microcellular process was introduced as the foaming molding method.

#### 3.1. The effect of process conditions on rim thickness of the textile roller of PBT with glass fiber by conventional injection molding

According to the sprue runner system of the mold (Fig. 4). The gates 3 and 5 (Fig. 2) are far from the runner as compared to the other gates on the up right cavity. So there is an unbalanced melt flow problem around this area. Fig. 6 shows the rim thickness of the roller by conventional molding. The maximum thickness is 6.075 mm on gate 11. The thickness variation is more than 0.10 mm, and points 4 and 5 have the least thickness.

#### 3.2. The effect of process conditions on rim thickness of the textile roller of PBT with glass fiber by microcellular injection molding

It needs certain time to make the microcellular injection molding stable when the supercritical fluid is introduced into the barrel. Parts are sampled after half an hour of operation to make sure the cell is uniform. Fig. 7 shows the rim thickness variation of the glass fiber filled PBT by

microcellular injection molding. The thickness variation is around 0.04 mm, which is on the margin of the specification, and the thinnest occurs at point 5. The thickness trend is similar to that of solid molding but the thickness variation is smaller for microcellular molding. However the maximum thickness occurs at point 12 (weld-line position) and the value is 6.27 mm. This is larger than that by conventional injection molding and it is caused by the expansion of the cell whereas it is compression on conventional injection molding. So the shrinkage rate for microcellular injection molding is less than that of conventional injection molding.

#### 3.3. The effect of process conditions on rim thickness of the textile roller of PBT with mineral fiber by microcellular injection molding

Figs. 8–13 show the rim thickness variation of Wollastonite filled PBT by microcellular molding. From the curves observed, the thickness variation of Wollastonite filled PBT is smaller than that of glass fiber filled PBT, and the curves of the Wollastonite filled PBT are smoother than those of glass fiber filled PBT. For the process conditions used, only the MPP has the trend whereas the MPP is increased, the rim thickness variation is decreased. MPP is the driving force to make cells smaller.

Figs. 14 and 15 show the microstructure of the cell near the gate of glass fiber and Wollastonite fiber filled PBT. The cell structure of Wollastonite fiber filled PBT is more uniform than that of glass fiber filled PBT, and the cell size is around 10  $\mu\text{m}$ .

The large rim thickness variation of glass fiber filled PBT may be attributed to the non-uniform cell structure. For the shrinkage rate [12], the average thickness of solid glass filled, foamed glass fiber filled, and foamed Wollastonite filled PBT is 6.004, 6.243, and 6.256 mm respectively. The thickness on the mold is 6.40 mm. In turn, the shrinkage rate is 6%, 2.4%, and 2.2% for solid glass filled, foamed glass fiber filled, and foamed Wollastonite filled PBT respectively.

The method to improve the rim thickness variation is changing the runner design as shown in Fig. 16. By this design, the melt has more balanced flow characteristics. Because the mold is too complex to modify, computer simulation, Modex3D [10], is used to simulate the flow characteristics of the old and modified design. Fig. 17 shows the rim shrinkage of the original and modified designs. It shows that the modified design has less shrinkage compared to the original design.

## 4. Conclusions

The effect of the process parameters on the rim thickness of glass fiber and Wollastonite filled PBT by conventional and

Table 1  
Process parameters for microcellular injection-molding process of the textile roller

	1	2	3
Melt temp. ( $^{\circ}\text{C}$ )	255	265	275
Injection speed ( $\text{cm}^3/\text{s}$ )	130	140	150
Shot size ( $\text{cm}^3$ )	39	41	43
MPP (bar)	130	140	150
SCF level (%)	0.18	0.28	0.38
Mold temp. ( $^{\circ}\text{C}$ )	40	50	60



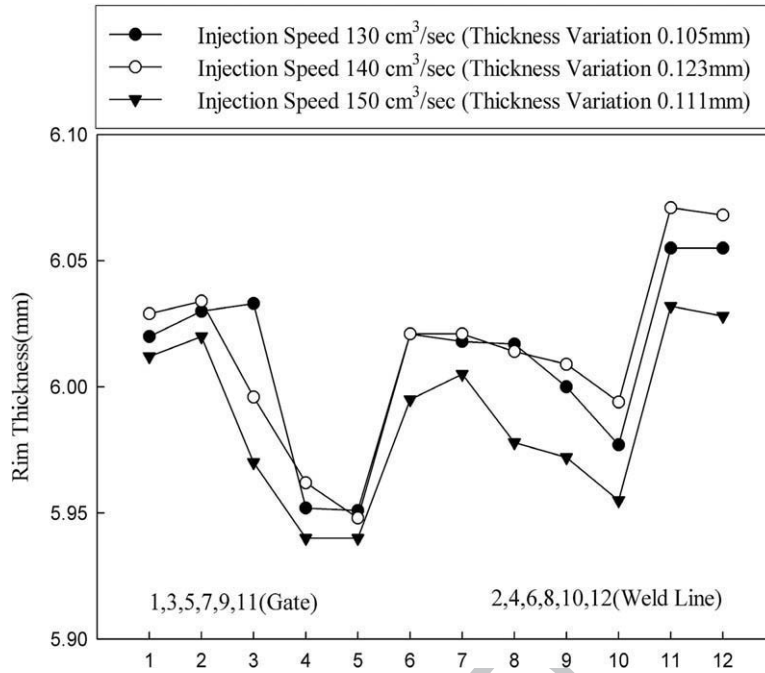


Fig. 6. Rim thickness variation vs. injection speed for solid glass fiber filled PBT.

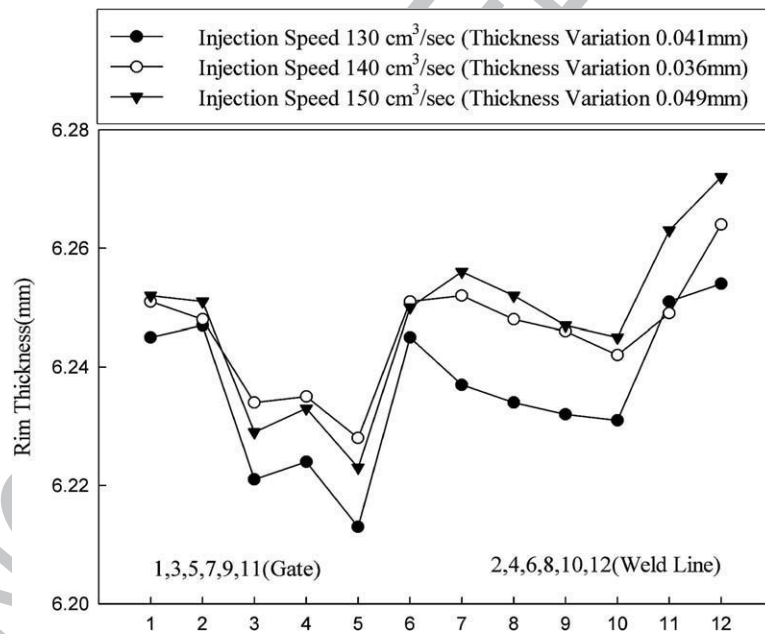


Fig. 7. Rim thickness variation vs. injection speed for foamed glass fiber filled PBT.

163 microcellular injection-molding process has been conducted. It  
 164 has been found that:

- 165 (1) For the rim thickness, microcellular injection molding has
- 166 smaller thickness variation than conventional molding.
- 167 (2) The textile roller has more uniform thickness with
- 168 Wollastonite filled PBT than glass filled PBT.
- 169 (3) Parts have less shrinkage by microcellular injection
- 170 molding compared to that by conventional molding.

- (4) Wollastonite filled PBT has more uniform cell struc- 171
- ture but lower shrinkage rate than that of glass filled 172
- PBT. 173

#### Acknowledgment 174

This work was supported by National Science Council of 175  
 Taiwan under contract # 94-2622-E231-004-CC3. 176

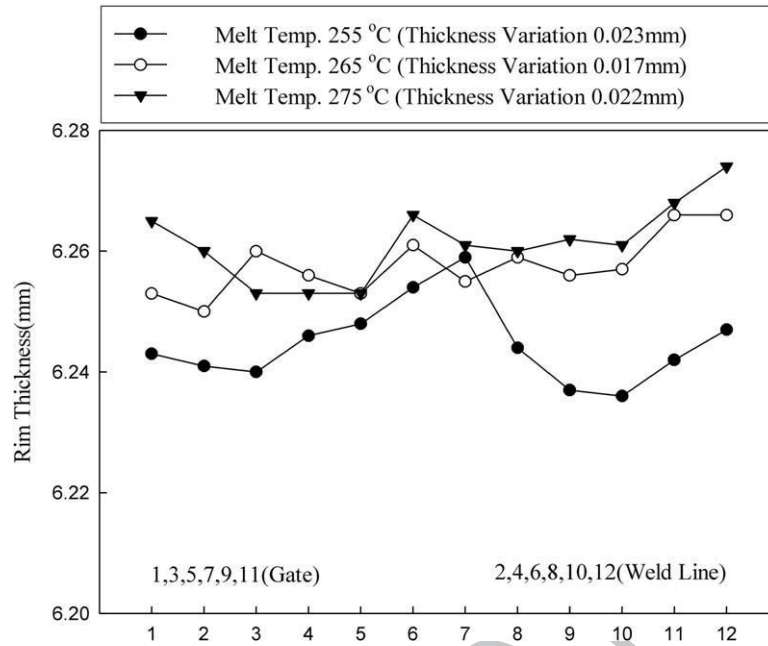


Fig. 8. Rim thickness variation vs. melt temperature for foamed Wollastonite fiber filled PBT.

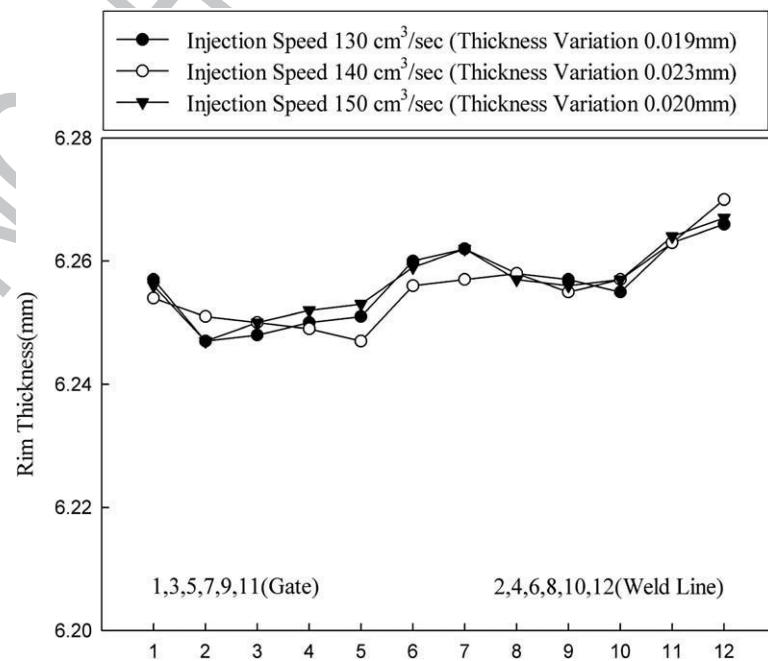


Fig. 9. Rim thickness variation vs. injection speed for foamed Wollastonite fiber filled PBT.

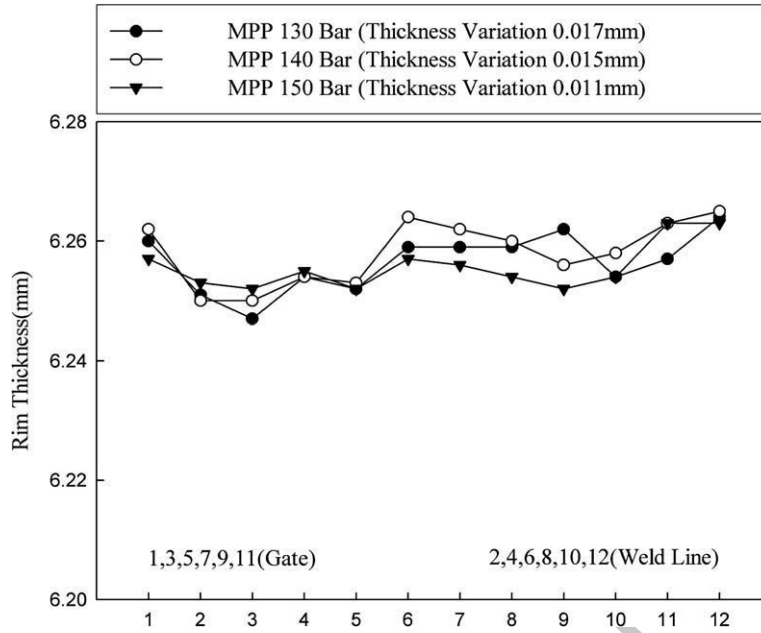


Fig. 10. Rim thickness variation vs. MPP for foamed Wollastonite fiber filled PBT.

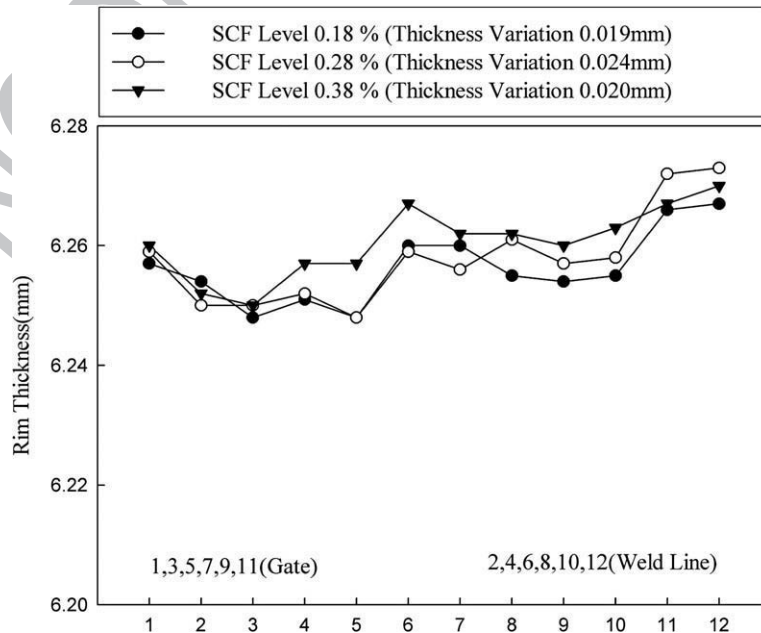


Fig. 11. Rim thickness variation vs. SCF level for foamed Wollastonite fiber filled PBT.

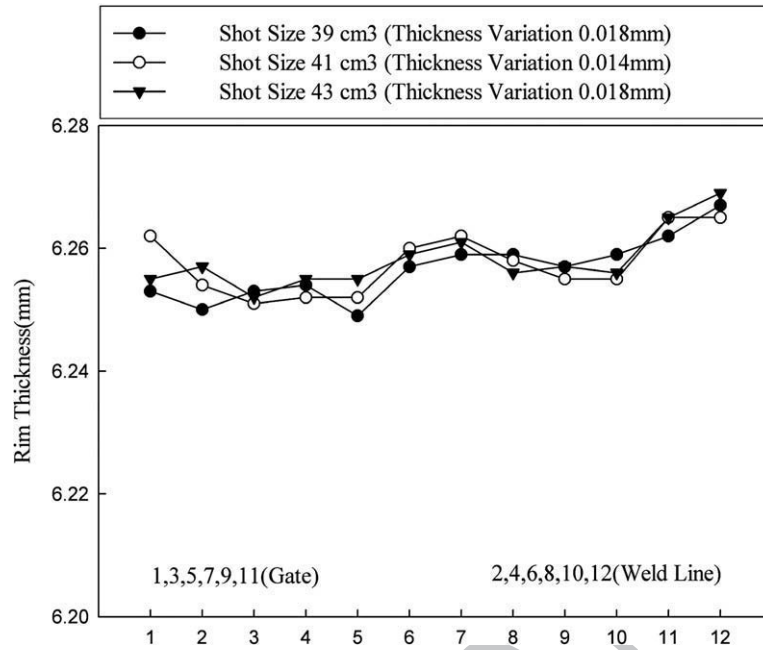


Fig. 12. Rim thickness variation vs. shot size for foamed Wollastonite fiber filled PBT.

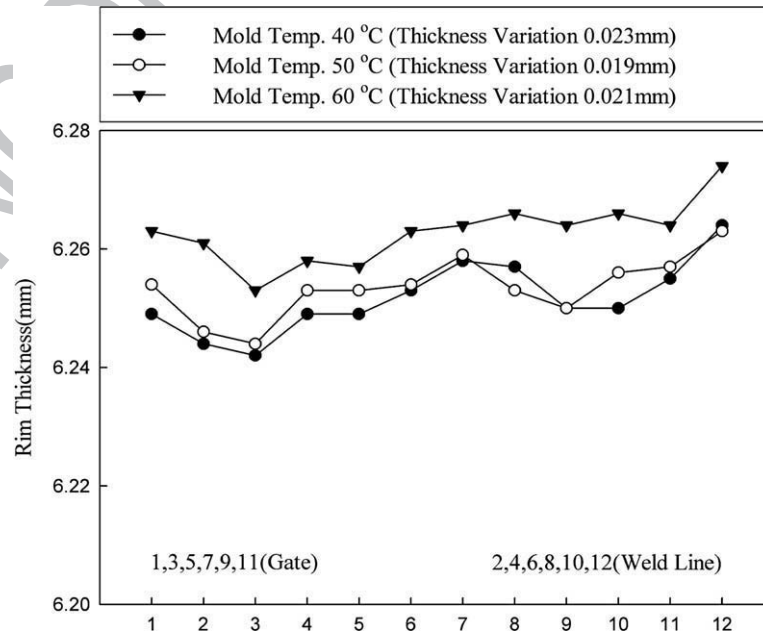


Fig. 13. Rim thickness variation vs. mold temperature for foamed Wollastonite fiber filled PBT.

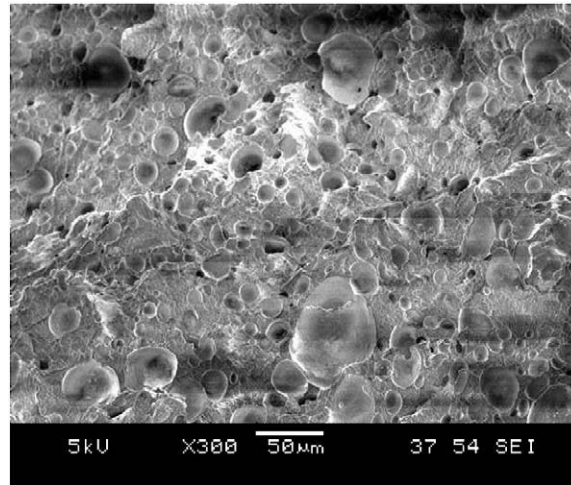


Fig. 14. The cell structure of the glass fiber filled PBT near the gate.

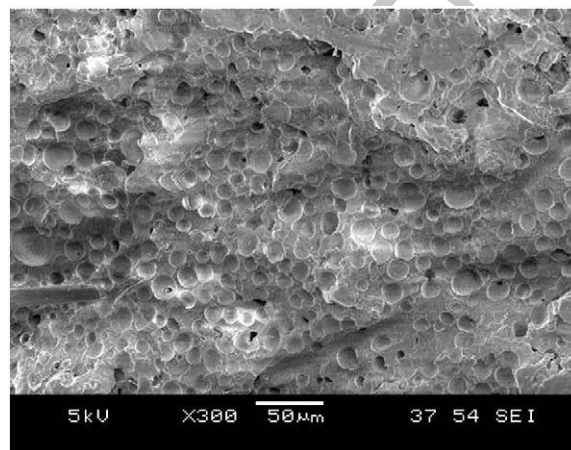


Fig. 15. The cell structure of the Wollastonite fiber filled PBT near the gate.

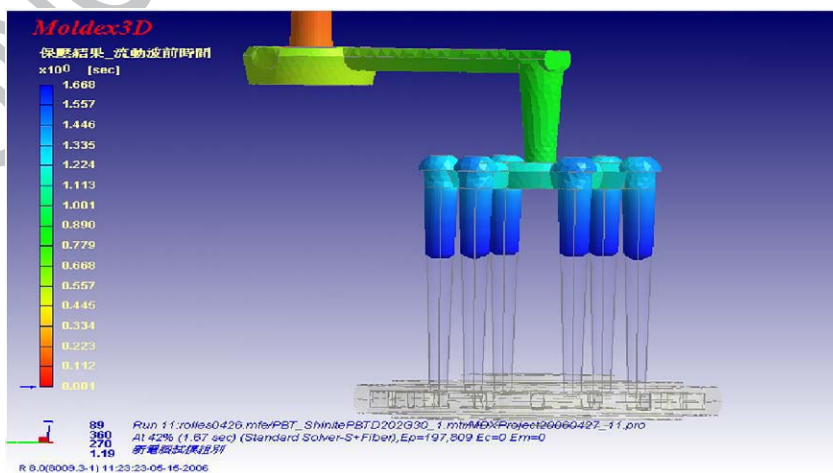


Fig. 16. More balanced design of the runner system.



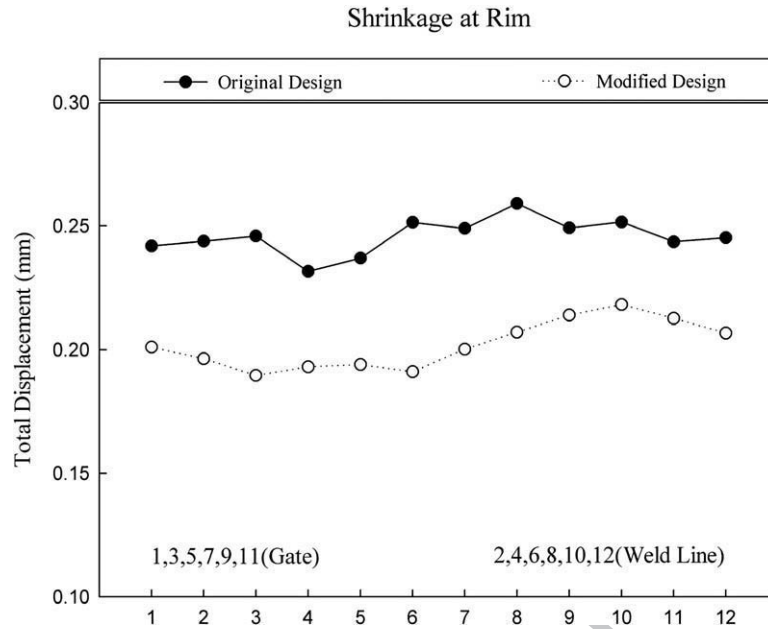


Fig. 17. Comparison of shrinkage at rim of the original and modified designs.

## References

- 177
- 178 [1] V. Martini, J.E., Nam. P. Suh, F.A. Waldman, U.S. Patent No. 4,473,665, 1984.
- 179
- 180 [2] Jonathan S. Colton, Nam P. Suh, Nucleation of microcellular foam: theory and practice, *Polymer Engineering and Science* 27 (7) (1987) 500–503.
- 181
- 182 [3] J.E. Martini, F.A. Waldman, N.P. Suh, Microcellular closed cell foams and their method of manufacture, *SPE ANTEC Tech. Papers*, 1982, pp. 674–678.
- 183
- 184 [4] W.C. Bushko, V.K. Stokes, Solidification of thermoviscoelastic melts. Part II: effects of processing conditions on shrinkage and residual stresses, *Polymer Engineering and Science* 35 (4) (1995) 365–373.
- 185
- 186 [5] W.C. Bushko, V.K. Stokes, Solidification of thermoviscoelastic melts. Part 3: effects of mold surface temperature differences on warpage and residual stresses, *Polymer Engineering and Science* 36 (3) (1996) 322–331.
- 187
- 188 [6] S.J. Liao, D.Y. Chang, H.J. Chen, L.S. Tsou, J.R. Ho, H.T. Yau, W.H. Hsieh, Optimal process conditions of shrinkage and warpage of thin-wall parts, *Polymer Engineering and Science* 44 (5) (2004) 917–929.
- 189
- 190
- 191
- 192
- 210
- 193 [7] A. Kramschuster, R. Cavitt, D. Ermer, Z. Chen, L.-S. Turng, Quantitative study of shrinkage and warpage behavior for microcellular and conventional injection molding, *Polymer Engineering and Science* 45 (10) (2005) 1408–1419.
- 194
- 195
- 196
- 197 [8] S.S. Hwang, Z.S. Ke, The dimensional stability of a microcellular injection molded gear shaft, *International Communications in Heat and Mass Transfer*, (in press).
- 198
- 199
- 200 [9] U. S. geological survey minerals information, *Mineral Yearbook, Metals and Mineral*, vol. 1, 1995, Reston, VA.
- 201
- 202 [10] Modex3D user manual, CoreTech System Co. Ltd, Hsinchu, Taiwan, 1998 (in Chinese).
- 203
- 204 [11] S.C. Chen, K.F. Hsu, K.S. Hsu, Simulation of the melt front advancement in injection molded plate with a rib of semicircular cross section, *Numerical Heat Transfer. Part A, Application* 28 (1) (1995) 121–129.
- 205
- 206
- 207 [12] S.C. Chen, N.T. Chen, K.S. Hsu, Simulation and verification of the secondary gas penetration in a gas-assisted-injection molded spiral tube, *International Communications in Heat and Mass Transfer* 22 (3), (1995) 319–328.
- 208
- 209
- Q2
- Q3